

## Effect of nitrogen on band alignment in HfSiON gate dielectrics

S. Sayan, N. V. Nguyen, and J. Ehrstein<sup>a)</sup>

Semiconductor Electronics Division, National Institute of Standards and Technology, Gaithersburg, Maryland 20899

J. J. Chambers, M. R. Visokay, M. A. Quevedo-Lopez, and L. Colombo

Silicon Technology Development, Texas Instruments Incorporated, Dallas, Texas 75243

D. Yoder, I. Levin, and D. A. Fischer

Ceramics Division, National Institute of Standards and Technology, Gaithersburg, Maryland 20899

M. Paunescu, O. Celik, and E. Garfunkel

Department of Chemistry, Rutgers University, Piscataway, New Jersey 08854

(Received 24 June 2005; accepted 27 September 2005; published online 16 November 2005)

Nitridation of HfSiO films improves certain physical and electrical properties—when using gate stack layers—such as their crystallization temperature and their resistance to interdiffusion. We have studied the band alignment of HfSiO and HfSiON films by soft x-ray photoemission, oxygen *K*-edge x-ray absorption, and spectroscopic ellipsometry. Nitridation of HfSiO reduced the band gap by  $1.50 \text{ eV} \pm 0.05 \text{ eV}$ , and the valence- and conduction-band offsets by  $1.2 \text{ eV} \pm 0.1 \text{ eV}$  and  $0.33 \text{ eV} \pm 0.05 \text{ eV}$ , respectively. Although the band-gap reduction should lead to increased leakage, the barrier heights are still sufficient for proposed near-future complementary metal-oxide-semiconductor applications. © 2005 American Institute of Physics.

[DOI: 10.1063/1.2135390]

The need for a high permittivity (high- $\kappa$ ) material for future metal-oxide-semiconductor (MOS) field effect transistors, is clear.<sup>1</sup> In order to replace SiON with a high- $\kappa$  dielectric, one of the primary requirements is that both valence- and conduction-band offsets of the material (with respect to the silicon band edges) should preferably be greater than 1 eV. Hafnium-silicon-based dielectrics exhibit a variety of desirable properties relative to other high- $\kappa$  dielectric alternatives, including their thermal stability, moderately high permittivity, and stability against crystallization.<sup>2,3</sup> In addition to appropriate physical properties, they also show many of the electrical characteristics needed for complementary MOS gate stack applications.<sup>2,3</sup> Nitrided HfSiO (herein designated as HfSiON) has also been extensively examined. Nitrided films show improved thermal stability, inhibited crystallization, improved electrical and dielectric properties, and decreased dopant, oxygen, and silicon interlayer diffusion when compared to hafnium silicates.<sup>4-7</sup>

Ikarashi *et al.*<sup>8</sup> characterized the effect of nitridation on the band gap of HfSiO using electron energy loss spectroscopy (EELS), and reported that the band gap of HfSiO was reduced by about 2 eV upon nitridation. The measured band gap of nitrided HfSiO was less accurate due to the fact that the low-loss structure was in the vicinity of the zero-loss tail, while the band gap of HfSiO could be more accurately measured.

Although there have been reports, as noted above, of the significant materials improvements that nitridation enables, the effect of nitrogen inclusion on the electronic structure of HfSiO, in general and on the valence and conduction band offsets in particular, has not been reported in detail. In this letter, we focus on valence- and conduction-band offsets, as

well as the optical band gaps of HfSiO and their nitrided derivatives.

Hafnium silicon oxide films were deposited by chemical vapor deposition methods directly on *n*-type silicon (100) substrates. High-resolution transmission electron microscopy (HRTEM) (not shown) combined with spatially resolved EELS (not shown) confirmed the amorphous nature of the as-deposited HfSiO films. HRTEM also revealed the presence of an interfacial silicon oxide layer having a thickness of 12 Å. Nitridation was accomplished through a postdeposition treatment that incorporated ~10 at. % N. All samples were annealed at 1000 °C in nitrogen. The generic formula of HfSiO can be represented as  $(\text{HfO}_2)_{1-x}(\text{SiO}_2)_x$ , and the silicates reported here are 60 mol % ( $x=0.60$ ). Vacuum ultraviolet (VUV) spectroscopic ellipsometry (SE) measurements were performed using a commercial instrument with a spectral range of 1.5 eV to 8.5 eV in steps of 0.02 eV. A four-phase model consisting of a silicon substrate, a SiO<sub>2</sub> interfacial oxide layer (determined to be 12 Å thick by HRTEM), a HfSiON film, and an air ambient was employed to extract the real and imaginary parts of the dielectric functions ( $\epsilon = \epsilon_1 + i\epsilon_2$ ).

Soft x-ray photoemission measurements were performed at the National Synchrotron Light Source (NSLS) at the Brookhaven National Laboratories on the U8B Beamline using photon energies from 120 eV to 400 eV. Samples for XPS measurements had HfSiON layers approximately 15 Å thick. The oxygen *K*-edge x-ray absorption spectroscopy (XAS) measurements were performed at NSLS on the U7A Beamline using the total electron yield mode. Samples for XAS, and also for SE, measurements had HfSiON layers approximately 40 Å thick.

Figure 1(a) presents the real ( $\epsilon_1$ ) and the imaginary ( $\epsilon_2$ ) parts of the dielectric function of the HfSiO and HfSiON films as determined by SE. Tauc plots (not shown) indicate

<sup>a)</sup>Electronic mail: jehrs@nist.gov

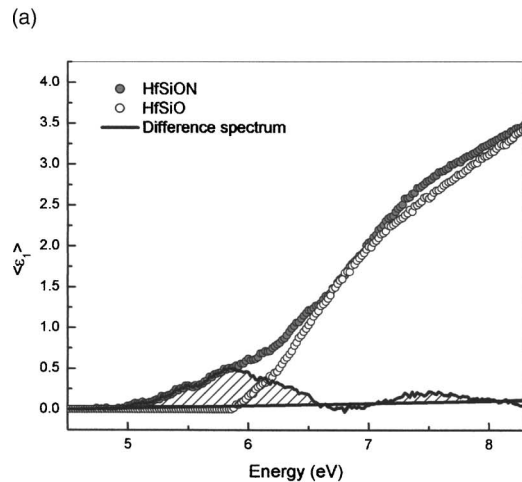
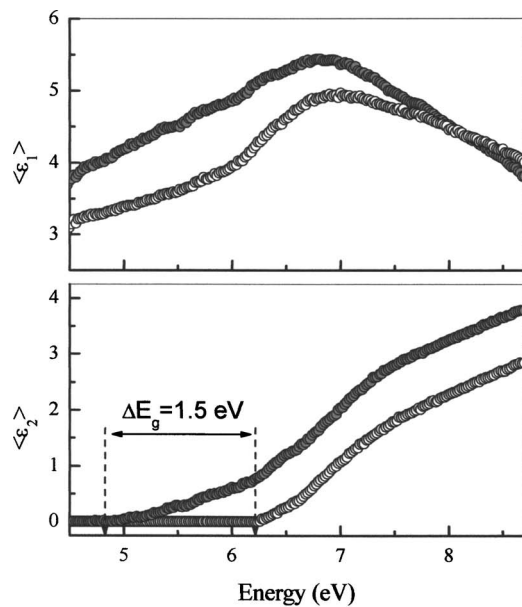
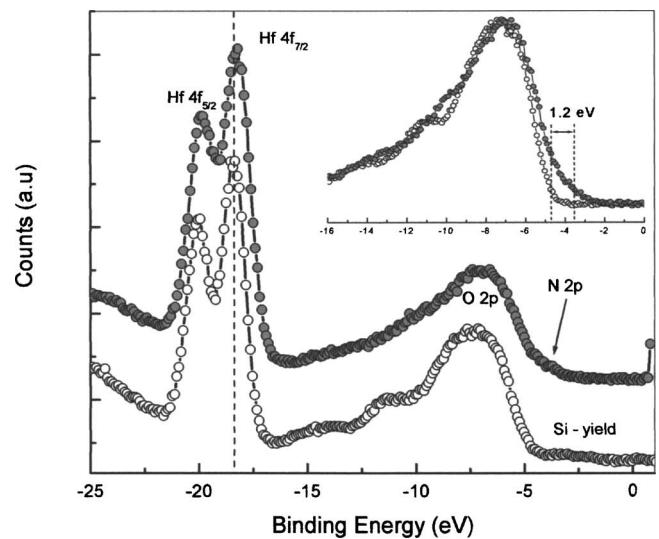


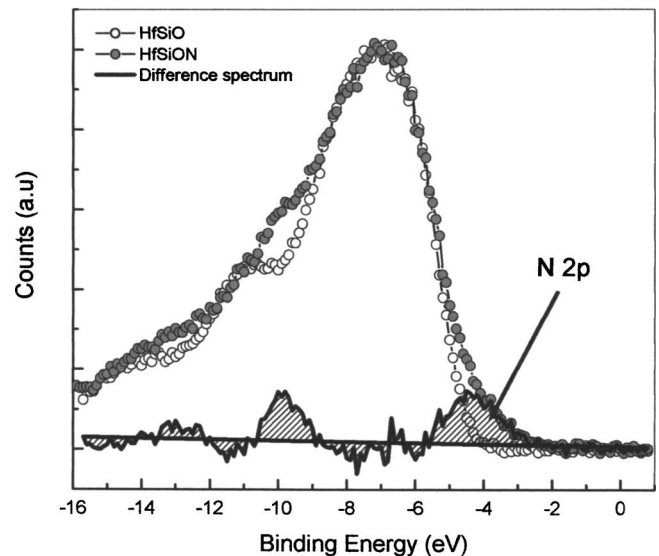
FIG. 1. (a) The real ( $\epsilon_1$ ) and imaginary ( $\epsilon_2$ ) part of the dielectric functions of HfSiO (squares) and HfSiON (circles) resulting from VUV-SE data following a four-phase modeling. (b) The difference spectrum of the imaginary ( $\epsilon_2$ ) part of the dielectric functions for HfSiO (squares) and HfSiON (circles). HfSiO dielectric function is shifted arbitrarily to align with that of the HfSiON, and spectral subtraction (solid line) has been performed.

optical band gaps of  $6.20 \text{ eV} \pm 0.05 \text{ eV}$  and  $4.70 \text{ eV} \pm 0.05 \text{ eV}$  for the HfSiO and HfSiON, respectively. Thus, the nitridation in the films reduced the effective optical band gap by  $1.50 \text{ eV} \pm 0.07 \text{ eV}$ . Figure 1(b) shows the difference spectrum of the imaginary ( $\epsilon_2$ ) part of the dielectric functions for the two materials (with and without N). The difference can be attributed to the nitrogen  $2p$  levels, as will be explained in more detail below.

Figure 2(a) shows the valence-band photoelectron spectra of these two films. The intense features in the 17 eV to 20 eV region corresponds to the Hf  $4f$  spin-orbit doublets. The curve fitting was performed after a Shirley background subtraction. A pair of Gaussians was used to model the Hf  $4f$  doublet representing the spin-orbit splitting of the  $4f$  level. The spin-orbit splitting was found to be 1.66 eV, and the intensity ratio was  $\sim 4:3$ , in agreement with the expected theoretical ratio. The binding energies of the Hf  $4f_{7/2}$  peaks were  $18.35 \text{ eV} \pm 0.05$  and  $18.47 \text{ eV} \pm 0.05 \text{ eV}$  for Hf in HfSiON and HfSiO, respectively. The bands in the 4 eV to 12



(a)



(b)

FIG. 2. (a) The valence-band photoelectron spectra of HfSiO (squares) and HfSiON (circles). The intense features in the 17 eV to 20 eV region is the Hf  $4f$  spin-orbit doublets. Dashed line is drawn to serve as a guide for the eyes. Inset is a close-up on the valence-band regions showing difference in the band details. (b) The valence-band spectra of HfSiO (squares) and HfSiON (circles). HfSiO valence band is shifted arbitrarily to align with that of the HfSiON to enable spectral subtraction (solid line). Note the differences in the valence-band fine structures due to presence of nitrogen states.

eV region are associated primarily with the oxygen and nitrogen  $p$ -like states. The fine structure of this band for the HfSiO is smeared out. For the identification of the nitrogen bands, the HfSiO spectrum was shifted to align with that of the HfSiON, and spectral subtraction was performed as shown in Fig. 2(b). One interesting point concerning the difference spectrum is that the positive trace is not counterbalanced with the negative trace area. This may mean that the addition of nitrogen into the silicate network may not be a substitution process.

Since the total spectrum is rather a complex function of thickness, profile, and composition, the deconvolution process is not straightforward. Two possible ways to understand the N incorporation are: (i) As a substitution reaction in which three O atoms are removed from the film for every

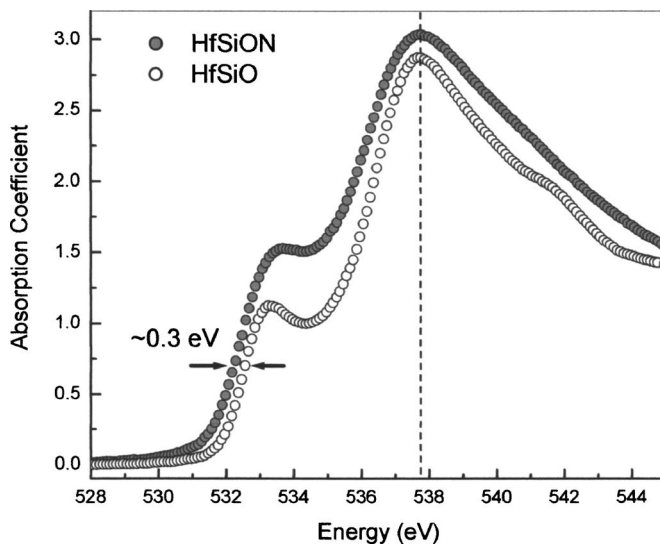


FIG. 3. The oxygen  $K$ -edge x-ray absorption spectra of HfSiO (squares) and HfSiON (circles). A difference of about 0.3 eV toward lower energies is observed in oxygen  $K$ -edge x-ray absorption spectra between HfSiO and HfSiON.

two N atoms incorporated, or (ii) as a growth reaction in which N diffuses to a buried interface, forming a  $\text{Si}_x\text{N}_y$  or  $\text{SiO}_x\text{N}_y$  layer.

The band edges are determined using the conventional method of linear extrapolation of the valence- and/or conduction-band leading edge to the background intensity level. Although this method is relatively straightforward for the valence-band edge of HfSiO, it cannot be applied directly to HfSiON, since the edge does not exhibit a linear shape or portion. Gaussian-modeled nitrogen states are assumed, and the edge is defined as the energy at the  $1\sigma$  level of the Gaussian distribution. Nitrogen reduces the valence band of HfSiON, and the valence-band offset difference between the HfSiO and HfSiON is found to be  $1.2 \text{ eV} \pm 0.1 \text{ eV}$ . The small intensity of the N  $2p$  peak resulting from the low concentration of N ( $[\text{N}] \sim 10 \text{ at. \%}$ ) in the film may be the main source of error in the definition of the band edge for HfSiON. Other methods of modeling the edge of the oxynitride would result in a change from 0.1 eV to 0.2 eV, although the trends would remain.

The O  $K$ -edge XAS near-edge structure of Hf-based metal oxides (Fig. 3) are dominated by the transitions into unoccupied final Hf  $5d$  states hybridized with O  $\pi$ -states. We use this information to assess the energy position of the Hf  $5d$  states in the different Hf-based metal oxides. A differ-

ence of about  $0.33 \text{ eV} \pm 0.04 \text{ eV}$  toward lower (shallower) energies is observed for the HfSiON (when compared with that of the HfSiO).

The incorporation of nitrogen into the HfSiO network reduces the effective band gap significantly. The valence-band offset is reduced by  $1.2 \text{ eV} \pm 0.1 \text{ eV}$  due to the presence N  $2p$  states which lie above that of O  $2p$  states. The conduction-band offset is also reduced, however to a lower extent, by about  $0.33 \text{ eV} \pm 0.04 \text{ eV}$ . This finding can be attributed to the lower symmetry around the hafnium cation and/or further splitting of Hf  $d$  states. The value obtained for the valence-band offset difference between the two systems is consistent with theoretical results for HfO<sub>2</sub> and Hf<sub>8</sub>O<sub>10</sub>N<sub>4</sub> reported by Shang *et al.*<sup>9</sup>

Incorporation of nitrogen into HfSiO reduced the optical band gap of the material by 1.50 eV, with the valence- and conduction-band offsets decreasing by 1.2 eV and 0.3 eV, respectively. Although nitridation of hafnium silicate has several materials advantages, such as increasing the crystallization temperature and reducing the interdiffusion between the different gate stack layers, inclusion of nitrogen in the hafnium silicate network reduces the valence- and conduction-band offsets. However, these offsets result in barrier heights that are still sufficient to make HfSiON a viable high- $\kappa$  for gate dielectric applications while taking advantage of the improved physical and electrical properties.

The authors would like to acknowledge support the NIST Office of Microelectronic Programs, the SRC and Sematech for partial support of this work.

<sup>1</sup>International Technology Roadmap for Semiconductors (ITRS) (SEMATECH, Austin, TX, 2003).

<sup>2</sup>G. D. Wilk, R. M. Wallace, and J. M. Anthony, J. Appl. Phys. **87**, 484 (2000).

<sup>3</sup>G. D. Wilk, R. M. Wallace, and J. M. Anthony, J. Appl. Phys. **89**, 5243 (2001).

<sup>4</sup>M. R. Visokay, J. J. Chambers, A. L. P. Rotondaro, A. Shanware, and L. Colombo, Appl. Phys. Lett. **80**, 3183 (2002).

<sup>5</sup>M. A. Quevedo-Lopez, M. El-Bouanani, M. J. Kim, B. E. Gnade, R. M. Wallace, M. R. Visokay, A. LiFatou, J. J. Chambers, and L. Colombo, Appl. Phys. Lett. **82**, 4669 (2003).

<sup>6</sup>L. Miotti, K. P. Bastos, G. V. Soares, C. Driemeier, R. P. Pezzi, J. Morais, I. J. R. Baumvol, A. L. P. Rotondaro, M. R. Visokay, J. J. Chambers, M. Quevedo-Lopez, and L. Colombo, Appl. Phys. Lett. **85**, 4460 (2004).

<sup>7</sup>T. Watanabe, M. Takayanagi, K. Kojima, K. Sekine, H. Yamasaki, K. Eguchi, K. Ishimaru, and H. Ishiuchi, Tech. Dig. - Int. Electron Devices Meet. **2004**, 507.

<sup>8</sup>N. Ikarashi, M. Miyamura, K. Masuzaki, and T. Tatsumi, Appl. Phys. Lett. **84**, 3672 (2004).

<sup>9</sup>G. Shang, P. W. Peacock, and J. Robertson, Appl. Phys. Lett. **84**, 106 (2004).